Available online at www.sciencedirect.com
SCIENCE DIRECT®
Journal of Magnetic Resonance 177 (2005) 86–92
JMR Journal of Magnetic Resonance
www.elsevier.com/locate/jmr

A multifrequency EPR approach to travertine characterisation

F. Di Benedetto [a], G. Montegrossi [b,*], L.A. Pardi [c], A. Minissale [b], M. Paladini [d], M. Romanelli [e]

[a] *Museo di Storia Naturale, Università di Firenze, Via G. La Pira 4, I50121 Firenze, Italy*
[b] *Istituto di Geoscienze e Georisorse—CNR, Via G. La Pira 4, I50121 Firenze, Italy*
[c] *Istituto per i Processi Chimico-Fisici—CNR, Via G. Moruzzi 1, I56124 Pisa, Italy*
[d] *Dipartimento di Scienze della Terra, Università di Firenze, Via G. La Pira 4, I50121 Firenze, Italy*
[e] *Dipartimento di Chimica, Università di Firenze, Via della Lastruccia 3, I50019 Sesto Fiorentino, Italy*

Received 11 May 2005; revised 13 July 2005
Available online 18 August 2005

Abstract

The understanding of processes that give rise to travertine deposits is important. This is so because of its widespread use as decorative material, but more so in environmental studies due to the significance, by proxy, of travertine in climatology. In this paper, a multifrequency EPR spectroscopy study of the behaviour of an ubiquitary vicariant of Ca in calcite, Mn(II), is presented. EPR spectra were obtained from a natural sample at 9.5 (X-band), 95, 190, and 285 GHz, and interpreted through numerical simulation. An analysis of the distribution of the zero-field splitting interaction revealed the source of some unexpected spectral features in the width of the lines in the X-band. By contrast, the homogeneous broadening plays only a minor role. Moreover, field-dependent anisotropies of the Zeeman and hyperfine tensors were observed at higher frequency. On the basis of results garnered in this study, the ZFS interaction of Mn(II) has been ascribed to the microstructural anomalies of the Mn(II) distribution in calcite. This may be considered as the fingerprint of the physical–chemical conditions at the time of travertine deposition. As a consequence, X-band EPR spectroscopy represents a specific tool to investigate the genesis, and to check the homogeneity of Mn(II) distribution in travertines as well as in other calcite-based materials.

Keywords: Travertine; Multifrequency EPR; Mn(II); Carbonate; ZFS distribution

1. Introduction

Investigations of the physical and chemical conditions leading to the formation of travertine, and more generally to other rock deposits, have undergone a noticeable quantitative and qualitative development during the last few years [1]. Beyond the obvious interest that accrues to basic knowledge of formation mechanisms of travertine, this kind of investigation has become more popular due to the connections with other typically applied fields of research, such as: pollution, paleoclimatology, archaeometry, etc. Moreover, the availability of new techniques and the improvement of those extant engenders a deeper and more comprehensive characterisation of the physical and chemical properties of such deposits [2]. Among these, electron paramagnetic resonance (EPR) has been recently introduced in this field because of its high sensibility and selectivity, but also due to the degree of accuracy of the local-scale information achievable in mineral structures.

Finding generic relations between the spectral parameters and the conditions at the time of formation of rock material is a crucial point. Some effort has been devoted to establishing specific relationships in the case of travertine [1,2]. The widespread use of this stone as building material is due to its extreme variability in morphology,

* Corresponding author. Fax: +39 0 55 290312.
E-mail address: giordano@geo.unifi.it (G. Montegrossi).

1090-7807/$ - see front matter © 2005 Elsevier Inc. All rights reserved.
doi:10.1016/j.jmr.2005.07.009

colour, shape, etc., linked to the characteristics of the parent deposit.

Travertine originates from $CaCO_3$-saturated springs by chemical precipitation. Among other cations, it always contains a certain amount of Mn(II) as a substituent of Ca in the calcite lattice structure. The presence of Mn(II) ($S = 5/2$, $I = 5/2$) makes the stone suitable for studies by EPR measurements. The X-band spectrum of Mn-bearing carbonate material is characterised by the presence of at least 16 lines. Most of these appear to be variably indented or split; the six more intense lines are due to the six allowed hyperfine transitions of the Kramer central doublet, whereas the others are attributed to forbidden hyperfine transitions [3]. These spectral features have been extensively studied in the past by using perturbation theory [3–5]. It is noticeable that in some studies [6–10] the possibility has been taken into account that some hamiltonian parameter can be related to the 'history' and the features of the examined sample. Nonetheless, no multifrequency studies of Mn(II) in calcite have been performed in order to discriminate the fundamental spectral features and to assess such hamiltonian parameters. In the present paper, the results of a multifrequency EPR investigation on a travertine sample are reported: this approach allowed a separate examination of the different interactions of the Hamiltonian. This suggests the use of the X-band spectral features as a specific investigation tool of generic conditions at the time of travertine precipitation.

2. Experimental and simulation procedures

A sample from the fossil travertine deposit of Papigno (PG) was selected for spectroscopic investigation. This travertine sample belongs to a recent meteogene deposit in the Tiber valley [1,11]. The Papigno deposit was most likely formed about 60 ka (unpublished age) by the Velino river at environmental temperature and pressure. The present absence of circulating water inside the Papigno deposit assures that no secondary calcite precipitation occurs, thus preventing any postdepositional event able to affect the crystal strain of the deposit [12] and consequently the interpretation of the spectroscopic data.

Conventional electron paramagnetic resonance spectroscopy (EPR) measurements were performed on powdered samples, in amorphous silica tubes. The spectra were registered both on free powders in the tube and on powders embedded in paraffin wax, to avoid magnetic orientation phenomena. Data were collected at room temperature using a Bruker ER 200D-SRC spectrometer operating at X-band (~9.5 GHz) interfaced with DS/EPR software to a PC for data acquisition and handling. The actual operating frequency value was determined using DPPH radical [2,2-di(4-tert-octyl-phenyl)-1-picrylhydrazyl, $g = 2.0037$] as an external standard. Due to the extremely narrow linewidth of Mn(II) spectra in calcite [5], particular care was taken in the choice of the instrumental field modulation and sweep rate. Owing to the fact that the spectral linewidth was found to vary under different field modulations, the operating conditions were varied until consistency of the resulting spectrum was achieved. The chosen set was: 0.05 mT modulation amplitude and 100 kHz modulation frequency. Scan speed was set to 0.2 mT per second.

The high-frequency EPR spectra were collected using the single pass technique, and a probe adapted for ultrawide band measurements. The source consists of a Gunn effect diode emitting at 95 GHz (W band) equipped with a doubler and a tripler to produce 190 and 285 GHz radiation. The magnet is a superconducting magnet (Oxford Instruments) operating at a maximum field of 12 T. The detector is a hot electron bolometer (QMC Instruments). The g_{iso} value was calculated to be 2.0014 compared to DPPH, taken as 2.0037. A modulation amplitude of 0.01 mT and 5.3 kHz modulation frequency set were appropriate values to observe reproducible spectra. At all frequencies (except the X-band) the spectral features, the linewidth, were found to depend also on the scan speed. In order to minimise this effect, and to obtain the most reliable spectrum, the slowest available scan speed, 0.5 mT per minute, was therefore chosen. Finally, pressed pellets of the powders mixed with KBr were prepared, in order to control the interactions of the crystallite with the intense magnetic fields.

Simulations were performed through different calculational approaches, in order to obtain the closest agreement between experimental and calculated spectra. The angular dependence of the line positions as a function of both the ZFS interaction and the incident microwave radiation frequency was evaluated through the third-order perturbative approach [5], implemented in a self-assembled FORTRAN program. The powder spectrum was obtained through weighted averaging of all possible crystallite orientations, assuming a Lorentzian linewidth. Owing to the fact that neither Zeeman nor hyperfine anisotropies are taken into account by this approach, two other procedures were also pursued.

Simulations of the experimental spectra were performed with the Weihe simulation software, SIM [13]. The SIM program has been specifically designed in order to leave the maximum freedom in the choice of the model for the spin system under investigation. The user supplies to the program the matrices corresponding to the different contributions of the Spin Hamiltonian. The number of introduced interactions and the orientation of the relative tensors can, therefore, be chosen opportunely. The program proceeds through numerical diagonalisation of the spin hamiltonian matrix, the retrieval of the transition fields, probabilities and

intensities, and, if requested, through a powder integration with a standard algorithm. The SIM program proved to be quite efficient for the simulation of very high field spectra due to the lack of any restraint in the allowed range of the spin hamiltonian and experimental parameters, in particular, the zero-field splitting, magnetic field, and frequency.

Simulations were also done by using a self-assembled computing program SPECMAG. The program sets up and diagonalises the spin hamiltonian matrix, where the electronic and nuclear Zeeman, hyperfine, quadrupolar, and fine interactions are taken into account. Eigenvalues and eigenvectors are found at chosen orientations of the reference system in the sample with respect to the Zeeman magnetic field direction; they were used to evaluate the positions and intensities of the allowed EPR transitions. The results were then interpolated to obtain the complete behaviour of the transitions in the selected field range. Finally, the supplied lineshape and linewidth are used, and interpolation in the range of orientations dictated by the site symmetry is accomplished. The results are summed together to obtain the powder spectrum.

3. Results

The room-temperature experimental EPR spectra of Mn(II) in the Papigno sample registered at all the frequencies (9.5, 95, 190, and 285 GHz, respectively) are reported in Fig. 1.

The X-band spectrum, similar to those reported in the literature [8], is composed by six main allowed hyperfine lines, the heights of which decrease by increasing the applied magnetic field B. A small indentation, present in the first and second line, increases up to a full splitting of the fifth and sixth lines into two upper and lower half-lines. Ten weaker lines can be observed within the main hyperfine sextet, corresponding to forbidden transitions [3]. No evidence has been revealed of lines corresponding to the outer transitions [14], i.e., to the four external sextets arising from the axial fine interaction, determined in calcite to be of the order of 8 mT [5]. Several X-band spectra of Mn(II) in calcite are reported in literature [2,5,8,9,14,15] occasionally presenting additional features: the microcrystalline marble and the powders of pure calcite, in fact, are characterised by a smaller linewidth, by the presence of few lines of the outer sextets, and by a smaller splitting to the sixth line; the trend of the intensity of the six main lines appears also different.

The W-band (95 GHz) spectrum, registered at the highest resolution (Fig. 1), comprises a well-resolved sextet of lines, whose intensity is asymmetric with respect to the spectrum centre; moreover, a small indentation appears in the two low-field lines (Fig. 2). No other

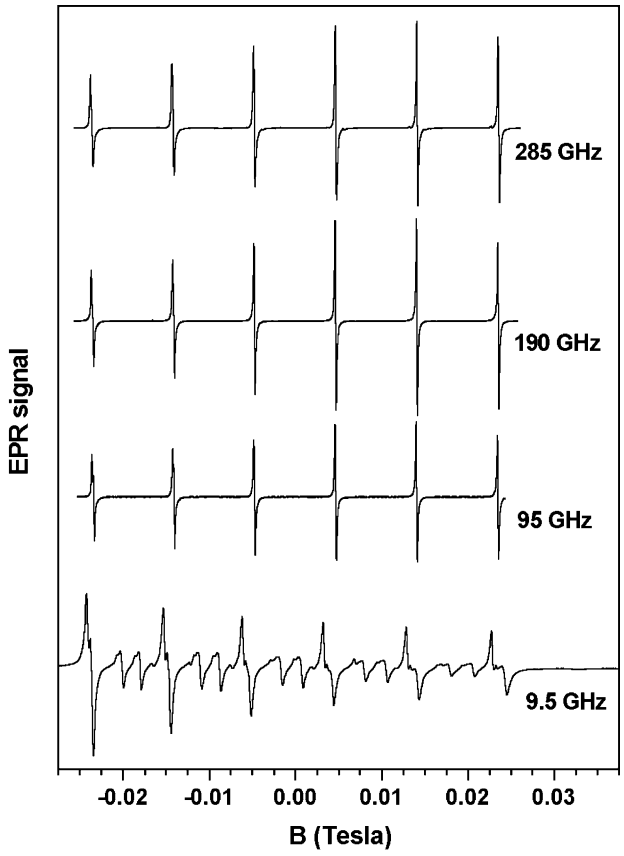

Fig. 1. Experimental EPR spectra at different frequencies, shown as the first derivative of the microwave absorption spectrum. Magnetic field values are normalised with respect to the free electron resonant field value ($g = 2$).

minor lines (i.e., outer allowed lines and forbidden lines) have been detected inside and outside the shown range. The linewidth of each line of the spectrum is definitely smaller than those of the X-band spectrum. The spectra registered at 190 and 285 GHz do not reveal the presence of extra lines: the most relevant features of the W-band spectrum, i.e., the indentation and the intensity trend, are still present and substantially unmodified. Nevertheless, a detailed comparison of the lowest-field line of the sextet (Fig. 2) reveals the indentation to be less evident, even if always appreciable, at higher frequencies, and a modification of its height from the baseline. Moreover, an evident shift of the line centre with increasing the applied frequency can be observed. Small shifts have been detected for all the other five lines, as shown in Fig. 3. The low-field lines present negative shifts, whereas high-field lines do the opposite. Small variations of the linewidth appear among the three high-frequency spectra (Fig. 4): the lower the field, the broader the lines.

Simulations of the experimental spectra are shown in Fig. 5, with the best-fit parameters listed in Table 1. In order to obtain consistent and reliable parameter values, the simpler high-frequency spectra were simulated first.

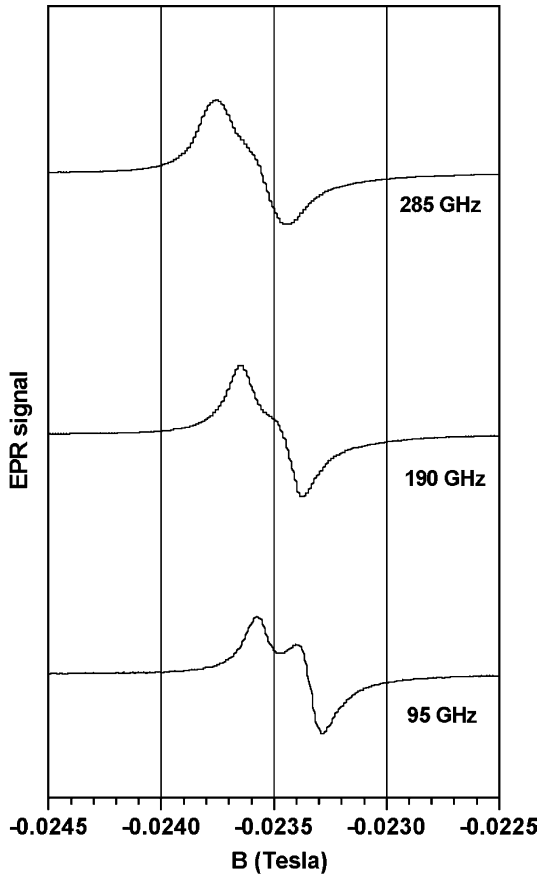

Fig. 2. Detail of the first line of the high-frequency EPR spectra of Fig. 1. Magnetic field values are normalised with respect to the free electron resonant field value ($g = 2$).

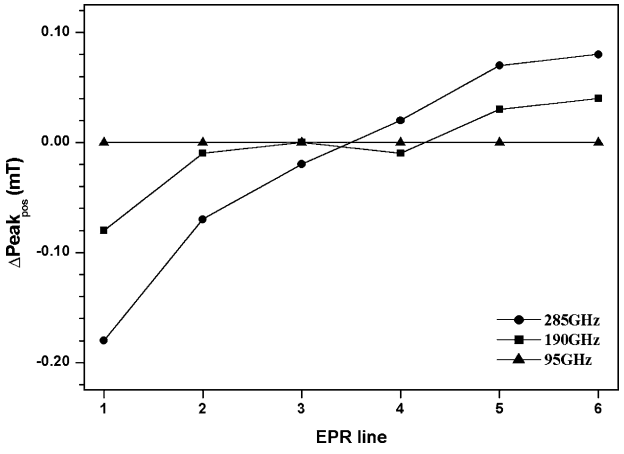

Fig. 3. Variation of the line positions with respect to the 95 GHz spectrum.

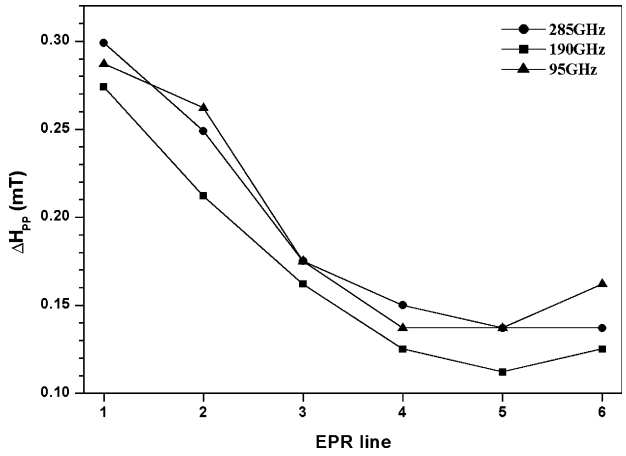

Fig. 4. Observed peak-to-peak linewidth for the high-frequency spectra.

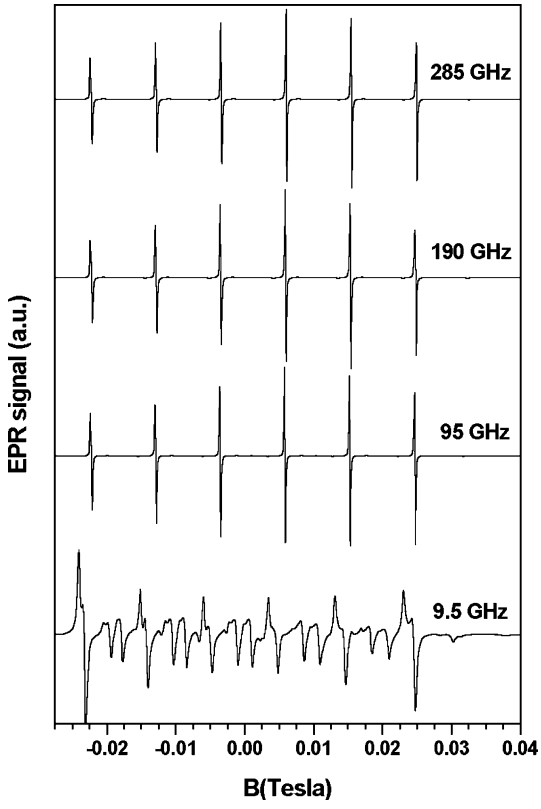

Fig. 5. Simulated EPR spectra at different frequencies. Hamiltonian parameters are reported in Table 1. Magnetic field values are normalised with respect to the free electron resonant field value ($g = 2$).

The simplest way to explain both the relevant experimental features, i.e., intensity trend and indentation, is the assumption of a small hyperfine anisotropy for Mn(II) in a distorted octahedral coordination [16]. The best-fit simulations resulted in a close reproduction of both the indentation and the intensity trend, but miss the position of the third, fourth, and fifth lines of ~0.1 mT. The possible presence of a small, but significant, Zeeman anisotropy, therefore, was taken into account.

The best-fit parameters indicate that an anisotropy of both the Zeeman and hyperfine tensors is able to reproduce correctly the asymmetric intensity pattern and the

Table 1
Best-fit Hamiltonian parameters used in the simulations of EPR spectra

	9.5 GHz	95 GHz	190 GHz	285 GHz
g_x	2.00140[a]	2.00132(1)	2.00132(1)	2.00132(1)
g_y	2.00140[a]	2.00132(1)	2.00132(1)	2.00132(1)
g_z	2.00140[a]	2.00140(1)	2.00135(1)	2.00134(1)
a_x (mT)	9.35(1)	9.35(1)	9.35(1)	9.40(1)
a_y (mT)	9.35(1)	9.35(1)	9.35(1)	9.40(1)
a_z (mT)	9.35(1)	9.43(1)	9.45(1)	9.48(1)
ΔH_x (mT)	0.40(1)	0.24(1)	0.24(1)	0.24(1)
ΔH_y (mT)	0.40(1)	0.24(1)	0.24(1)	0.24(1)
ΔH_z (mT)	0.70(1)	0.10(1)	0.10(1)	0.10(1)
D (mT)	9.85(5)	9.85[a]	9.85[a]	9.85[a]

[a] Not refined values.

indentation of the low-field lines, as well as the line positions. Both tensors are characterised by axial symmetry, with the parallel z-component greater than those of the perpendicular x and y components. The Zeeman anisotropy results in a fairly small correction, of the order of 0.04‰, whereas the hyperfine anisotropy is much larger, ~1%. The data of Figs. 3 and 4 confirm that a small v-dependent variation of the Zeeman or the hyperfine tensors (or both) should be present. At 190 GHz, in fact, a small decrease of the Zeeman anisotropy was necessary to fit the experimental spectrum, whereas at 285 GHz the hyperfine anisotropy was also slightly changed (Table 1). The $g_{\|}$ and $a_{\|}$ components have an opposite trend, with a decrease in the former and increase in the latter, with increasing operating frequency.

The computed linewidth values are small, $\Delta H_{av} < 0.2$ mT: the width of the parallel component is less than a half the width of the perpendicular component. No width variations are obtained by changing the frequency, thus suggesting that neither appreciable field dependence nor broadening due to field inhomogeneities occur. We remark that in order to simulate the complete experimental disappearance of the outer transition lines, a limitation of the θ range in the spatial averaging procedure of the simulation was necessary, θ being the angle between the magnetic field direction and the main crystallographic axis of the calcite particles. The largest reduced range compatible with the experimental observation was $15° < \theta < 75°$. This range is fully in agreement with the isoorientation caused by the volume reduction under pressure during pellet preparation, consistent with the usual rhombohedral crystal habitus.

No effects of the zero-field splitting occur appreciably in the high-frequency spectra of Mn(II)-bearing calcite [14]. Nevertheless, an attempt to study the modification of the spectral features under an increasing ZFS interaction was undertaken through a third-order perturbative approach. The splitting between the upper and lower half-lines, characteristic of the X-band spectrum, is due to the angular dependence of the line position through the ZFS effect. An axial D value >12 mT, somewhat larger than the values of Table 1, is required, in order to observe a small indentation at 95 GHz. Moreover, even larger values would be necessary to affect the spectra at 190 and 285 GHz. By contrast, ZFS values within the range 0–12 mT were found not to alter the spectral features of the high-field simulated spectra at all, a conclusion also obtained using the SIM software. The high-field simulations, therefore, do not need ZFS to be taken into account, and the D value is not refinable from these spectra.

The best-fit parameters of the high-frequency simulations were used as a basis set to simulate the X-band spectrum. However, the anisotropies of the Zeeman and hyperfine tensors gave results not compatible with the experimental line positions. Fully isotropic tensors were therefore chosen, in agreement with the results obtained with single crystal measurements [10]. The best-fit values for the width are definitely broader than the high-frequency values. The D value obtained, 9.85 mT, appears rather large when compared with literature data [5,7]. However, this value was necessary to fit the observed value of the highest-field line splitting, 1.82 mT (Figs. 1, 5, and 6), which is larger than the pure calcite value, 1.40 mT [5].

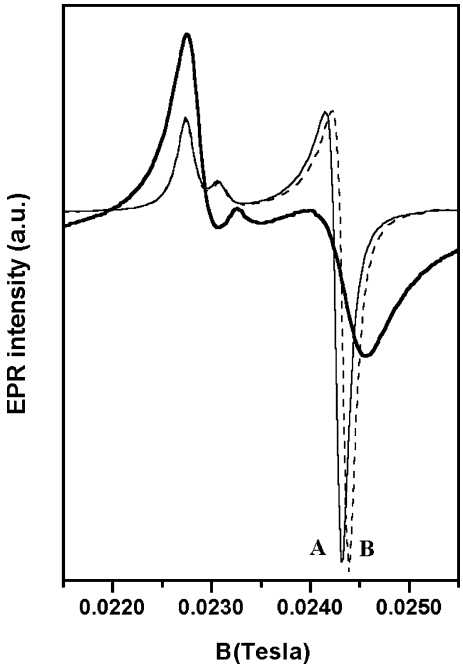

Fig. 6. Detail of the sixth line of the 9.5 GHz EPR spectrum of Fig. 1, together with two different simulated spectra: (A) $\Delta H = 0.2$ mT, $D = 9.63$ mT; (B) $\Delta H = 0.2$ mT, $D = 9.85$ mT. Magnetic field values are normalised with respect to the free electron resonant field value ($g = 2$).

4. Discussion

4.1. High-frequency spectra

The most striking result obtained from the high-frequency spectra is the presence of both the Zeeman and the hyperfine anisotropies. These anisotropies, indeed, are rather unusual for the d^5 Mn(II) ion, which has a $^6A_1$ ground state in the pure octahedral coordination [7]. Nevertheless, a small spin-allowed admixture between the ground and the first excited states via spin–orbit coupling is formally allowed in calcite, even if energetically unfavoured: the Ca site in calcite, in fact, has a non-cubic D_{3d} local symmetry.

Holuj and Kwan [16], in their EPR study of Mn in $Ca(OH)_2$ crystals, presented two distinct g-tensor components. This was in agreement with the crystal field assumptions, and the difference between the values reported was within the experimental uncertainty. By contrast, in the present study small but consistent anisotropies were revealed with high experimental accuracy.

The presence of variable anisotropy values in the three different high-frequency experiments and the full isotropy of the Zeeman and hyperfine tensors at the X-band suggest that the origin of the anisotropy is not related to the usual spin–orbit coupling term in the hamiltonian. In order to understand the nature of the field/frequency variations of the tensor components, the experimental linearity of the scanned field at the higher operating frequencies (95, 190, and 285 GHz) was carefully checked, resulting in confirmation of this observation (less than 0.1 mT of disagreement between the expected and registered values of B_0). Owing to the fact that no magnetic orientation of the crystallites was expected for the pellets used, the changes of the tensor components as a function of the operating frequency were ascertained to be a property of the sample and the existence of field-dependent terms of the spin hamiltonian operator, enhanced and/or revealed by the extremely narrow linewidth considered. To find the theoretical origin of this spectral feature is outside the goal of this paper. Nevertheless, we mention that Koster and Statz [17] developed a method for treating the interactions of a paramagnetic ion in a crystalline field different from the commonly used 'spin hamiltonian' method. In this framework, they found that, at high Zeeman fields, the six sublevels of a ^6S state ion do not exhibit a homogeneous behaviour. Namely, the energies of two of these show a linear dependence on the field, but those of the other four depend on the field with a factor that includes the square root of g parameters. At present, calculations are in progress to check this deviation from linearity as the source of the non-linear dependence on the field, as well as to evaluate its effects on the hyperfine tensor components.

4.2. X-band spectrum

The larger linewidth values and the dependence of the spectrum on the axial ZFS parameter, D, besides the isotropy of Zeeman and hyperfine tensors, distinguish the X-band from the high-frequency spectra. In the present spectrum, in fact, the linewidth and the trend of the intensity of central sextet appear to be quite different from those reported in literature for powders of finely ground calcite [5,9,14], whereas a resemblance is observed with the spectra of natural polycrystalline calcite-bearing materials [2,8,10]. Moreover, an evident difference between the experimental width of the upper and lower half-lines (Fig. 6) cannot easily be related to structural or broadening anisotropies. Even if these characteristics are known in the literature [5], several authors have pointed out the difference between the experimental spectra obtained on natural microcrystalline powders and on ground calcite macrocrystals. The former, in particular, appears broader and less resolved as concerns the half-line splitting. A different intensity pattern was also noted: in natural powders the intensity progressively decreases from the first line, whereas in ground calcite the two central lines are depleted with respect to the external ones [5]. These differences were observed also on single crystal spectra, and the existence of a zero-field splitting (ZFS) distribution was, therefore, inferred [10].

On the basis of the present high-frequency observations, no significant width variations are observed. At least they do not lead to values bigger than 0.2 mT. As a consequence, a large line broadening at X-band appears unlikely. On the contrary, the ZFS distribution origin can account for all the experimental evidence. It has to be noted, in fact, that small differences of the D parameter values result in an undetectable change in the position of the upper half-lines and in easily detectable changes in the position of the lower half-lines (Fig. 6). If a continuous distribution is considered, the observed pattern can be explained. Under these assumptions, therefore, not only the existence of the line broadening, but also its different effect on the upper and lower half-lines are justified. At high frequencies, if the D influence is not detectable, then also the variation induced by its distribution will be lost. The best-fit D value (Table 1) represents the mean value of the ZFS distribution, whereas ΔH parameters can be related to the half-value of the ZFS distributions range.

The presence of a ZFS distribution can be related to structural inhomogeneities, provided that the temperature and the other relevant physical and chemical parameters are constant (pH, chemical concentration of mineralising fluid, etc.). Vassilikou-Dova [10], in particular, gave evidence that a correlation between the frequent chemical inhomogeneity of calcite (i.e., sector zoning) and the existence of cation sites is not equivalent

at the local scale. Mn(II) ions, hosted in slightly different environments, would yield slightly different EPR spectra, the convolution of which can give rise to the experimental spectrum. It has to be pointed out that in natural travertines the stability of the physico-chemical factors is far from being constant. Indeed, the small variation of these factors points to the presence of residual structural strains caused by a fast precipitation from a supersaturated solution as the most probable explanation of the ZFS distribution.

5. Conclusions

The multifrequency spectra of the Papigno sample provided fundamental information not only for the full isotropy of the Zeeman and hyperfine tensors at the X-band, but also for the natural homogeneously broadened linewidth of the Mn(II) lines in calcite. This allows an interpretation of the large linewidth values at X-band to be attributed to inhomogeneous broadening caused by a ZFS distribution. Moreover, the field-dependent tensor anisotropy observed in all the high-frequency spectra may be considered as an important experimental basis for testing fine theoretical model of the magnetic field/paramagnetic ions interactions.

The inhomogeneous broadening of the line observed at X-band and thus the variability of the ZFS interaction, both linked to small structural anomalies of the Mn(II) crystal chemistry in calcite, can be considered as phenomenological markers of travertines. X-band EPR, therefore, provides a powerful tool to investigate the "fingerprints" of the physical–chemical conditions of the travertine deposition and to check its homogeneity within a given deposit.

Acknowledgments

The authors acknowledge G.P. Bernardini and B. Ninham for their critical revision of the text and V. Bercu for the high-frequency measurements. Two anonymous referees, who provided useful suggestions to improve the text, are also sincerely acknowledged. This work was carried out with the partial financial support of Italian CSGI. The HF^{2}EPR laboratory acknowledges the Interuniversitary Consortium for the Science and Technology of Materials (INSTM) and the National Research Council for financial support. The EC network SENTINEL, Contract No. HPRI-CT-2000-40022, is also acknowledged for the scientific collaboration and the technological cooperation.

References

[1] A. Minissale, Origin, transport and discharge of CO_2 in central Italy, Earth Sci. Rev. 66 (2005) 89–141.
[2] D. Kralj, J. Kontrec, L. Brečevic, G. Falini, V. Nöthig-Laslo, Effect of inorganic anions on the morphology and structure of magnesium calcite, Chem. Eur. J. 10 (2004) 1647–1656.
[3] B. Bleaney, R.A. Rubins, Explanation of some 'forbidden' transitions in paramagnetic resonance, Proc. Philos. Soc. 77 (1961) 103–112.
[4] V. Beltran-Lopez, J. Castro-Tello, EPR lineshapes in polycrystalline samples: $^6S_{5/2}$ ions in axial and cubic crystal fields, J. Magn. Reson. 39 (1980) 437–460.
[5] R.A. Shepherd, W.R.M. Graham, EPR of Mn^{2+} in polycrystalline dolomite, J. Chem. Phys. 81 (12) (1984) 6080–6084.
[6] E.R. Feher, Effect of the uniaxial stresses on the paramagnetic spectra of Mn^{2+} and Fe^{3+} in MgO, Phys. Rev. 136 (1A) (1964) 145–157.
[7] A. Abragam, B. Bleaney, in: Electron Paramagnetic Resonance of Transition Ions, Clarendon Press, Oxford, 1970, p. 700.
[8] J.A. Angus, B. Raynor, M. Robson, Reliability of experimental partition coefficients in carbonate systems: evidence for inhomogenous distribution of impurity cations, Chem. Geol. 27 (1979) 181–205.
[9] B. Fubini, F.S. Stone, Investigation of the vaterite-calcite transformation by ESR spectroscopy using Mn^{2+} ions as a tracer, J. Mater. Sci. 16 (1981) 2439–2448.
[10] A.B. Vassilikou-Dova, Characterisation of the crystal quality of calcites by electron paramagnetic resonance, Phys. Status Solidi B178 (1993) 465–476.
[11] A. Minissale, D. Kerrich, G. Magro, M.T. Murrell, M. Paladini, S. Rihs, N. Sturchio, F. Tassi, O. Vaselli, Geochemistry of Quaternary travertines in the region north of Rome (Italy): structural, hydrologic and paleoclimatic implications, Earth Planet. Sci. Lett. 203 (2002) 709–728.
[12] A.C. Lasaga, A. Luttge, Variation of crystal dissolution rate based on a dissolution stepwave model, Science 291 (2001) 2400–2404.
[13] J. Glerup, H. Weihe, Magnetic susceptibility and EPR spectra of μ-cyano-bis[pentaaminechromium(III)] perchlorate, Acta Chim. Scand. 45 (5) (1991) 444–448.
[14] T.R. Wildeman, The distribution of Mn^{2+} in some carbonates by electron paramagnetic resonance, Chem. Geol. 5 (1970) 167–177.
[15] D. Attanasio, The use of electron spin resonance spectroscopy for determining the provenance of classical marbles, Appl. Magn. Reson. 16 (1999) 383–402.
[16] F. Holuj, C.T. Kwan, Isotope effects in the ESR of Mn^{++} in $Ca(OH)_2$ and $Ca(OD)_2$, Phys. Rev. B 9 (1974) 3673–3677.
[17] G.F. Koster, H. Statz, Method of treating Zeeman splittings of paramagnetic ions in crystal fields, Phys. Rev. 113 (1959) 445–454.